

In-Film Bioprocessing and Immunoanalysis with Electroaddressable Stimuli-Responsive Polysaccharides

By Xiaohua Yang, Eunkyong Kim, Yi Liu, Xiao-Wen Shi, Gary W. Rubloff, Reza Ghodssi, William E. Bentley, Zeev Pancer, and Gregory F. Payne*

Advances in thin-film fabrication are integral to enhancing the power of microelectronics while fabrication methods that allow the integration of biological molecules are enabling advances in bioelectronics. A thin-film-fabrication method that further extends the integration of biology with microelectronics by allowing living biological systems to be assembled, cultured, and analyzed on-chip with the aid of localized electrical signals is described. Specifically, the blending of two stimuli-responsive film-forming polysaccharides for electroaddressing is reported. The first, alginate, can electrodeposit by undergoing a localized sol–gel transition in response to electrode-imposed anodic signals. The second, agarose, can be co-deposited with alginate and forms a gel upon a temperature reduction.

Electrodeposition of this dual polysaccharide network is observed to be a simple, rapid, and spatially selective means for assembly. The bioprocessing capabilities are examined by co-depositing a yeast clone engineered to display a variable lymphocyte receptor protein on the cell surface. Results demonstrate the in-film expansion and induction of this cell population. Analysis of the cells' surface proteins is achieved by the electrophoretic delivery of immunoreagents into the film. These results demonstrate a simple and benign means to electroaddress hydrogel films for in-film bioprocessing and immunoanalysis.

biosensing, genomics, and proteomics. Analogous efforts are underway to localize, culture, and analyze viable cells on-chip for applications that range from performing fundamental studies in cell biology to mimicking the multi-organ metabolism of drugs. Three themes appear to be emerging for the on-chip cultivation of cells. First, hydrogel films are generally preferred for replicating biological micro-environments and preserving labile biological functions (e.g., to maintain cell viability).^[1–7] Second, fabrication methods for patterning films often enlist convenient, spatiotemporally controllable stimuli. For instance, printing and photolithographic patterning employ mechanical and optical inputs,^[6,8–14] while there are growing efforts to use electrical stimuli to perform functions such as electroaddressing.^[15–33] Finally, biological materials and mechanisms may offer opportunities to “biofabricate” functional hydrogel films.^[34–41] For instance, stimuli-responsive biological polymers form hydrogels in response to mild stimuli, these hydrogel networks can be reversibly formed/broken, and there is

extensive biotechnological experience with biopolymer-based hydrogels (e.g., gelatin and agarose).

Recently, stimuli-responsive polysaccharides have been observed to be capable of electrodepositing at electrode surfaces in response to localized electrical signals.^[42,43] In most cases, these

1. Introduction

Technologies that allowed nucleic acids and proteins to be spatially localized and analyzed on-chip enabled remarkable progress in

[*] Prof. G. F. Payne, Dr. X. Yang, Dr. E. Kim, Dr. Y. Liu, Dr. X.-W. Shi, Prof. W. E. Bentley
Center for Biosystems Research
University of Maryland Biotechnology Institute
5115 Plant Sciences Building
College Park, MD 20742 (USA)
E-mail: payne@umbi.umd.edu
Prof. G. W. Rubloff
Department of Materials Science and Engineering
University of Maryland
College Park, MD 20742 (USA)

Prof. G. W. Rubloff, Prof. R. Ghodssi
Institute for Systems Research
University of Maryland
College Park, MD 20742 (USA)

Prof. R. Ghodssi
Department of Electrical and Computer Engineering
University of Maryland
College Park, MD 20742 (USA)

Prof. W. E. Bentley
Fischell Department of Bioengineering
University of Maryland
College Park, MD 20742 (USA)

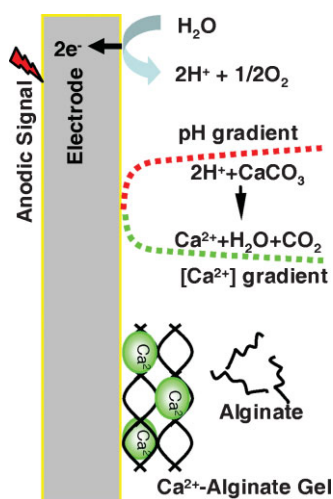
Prof. Z. Pancer
Center of Marine Biotechnology
University of Maryland Biotechnology Institute
Baltimore, MD 21202 (USA)

DOI: 10.1002/adfm.200902092

polysaccharides electrodeposit in response to electrochemically induced pH gradients that neutralize the polymer. For instance, the aminopolysaccharide chitosan undergoes gel formation at the cathode surface in response to a localized high pH that results in the conversion of its cationic ammonium groups into neutral amines.^[44–46] Similarly, the acidic polysaccharides alginate^[47,48] and hyaluronate^[49,50] were observed to electrodeposit at the anode surface in response to a localized low pH. An alternative mechanism for electrodepositing alginate films is illustrated in Scheme 1.^[51] In this case, insoluble CaCO_3 is suspended in a solution of sodium alginate. Anodic electrolysis reactions generate a pH gradient that causes the localized solubilization of Ca^{2+} , which then induces the formation of calcium alginate gels.

An important feature of polysaccharide electrodeposit is that it enables co-deposition—materials dissolved or suspended in the polysaccharide solution can be incorporated into the electro-deposited films. One of the initial reports of co-deposition involved the entrapment the glucose oxidase and gold nanoparticles for biosensor fabrication^[52] and these studies were rapidly extended to other systems and enzymes^[53–62] and to the co-deposition of a range of inorganic^[21,63] (e.g., carbon nanotubes^[64–67]) and organic nanoparticles.^[68] An alternative goal for co-deposition is to generate composite surface coatings.^[47,69–73] Two previous observations are particularly relevant to the current study. First, it was recently reported that the stimuli-responsive film-forming polysaccharide chitosan allowed the co-deposition of a second polysaccharide (heparin) that is unable to electrodeposit by itself but that confers distinct functions to the deposited film.^[74,75] Second, viable bacterial cells were co-deposited in Ca^{2+} -alginate films (using the mechanism of Scheme 1) and these cells could be grown, induced, and released (by dissolving the films with sodium citrate that binds Ca^{2+}).^[51]

The goal of the work reported here is to extend the capabilities of Ca^{2+} -alginate film bioprocessing by allowing the film-entrapped cells to be probed with immunoreagents (i.e., antibodies) that recognize cell surface proteins. Immunoanalysis of cell surface antigens is integral to a variety of techniques such as the



Scheme 1. Mechanism for calcium alginate electrodeposit. Electrolysis at the anode generates a pH gradient that triggers the localized release of calcium from insoluble CaCO_3 . This localized solubilization of Ca^{2+} induces the gelation of calcium alginate adjacent to the anode surface.

determination of blood type, the serotyping of pathogens, and the detection of cell surface biomarkers (e.g., for cancer diagnosis). A key requirement for immunoanalysis of film-entrapped cells is that the antibody-based immunoreagents must be capable of penetrating into the hydrogel network to access the cells. As will be shown, antibodies do not appear to diffuse or migrate into alginate gels. Thus, we investigated films prepared by the co-deposition of alginate with a second stimuli-responsive polysaccharide agarose.

2. Results and Discussion

2.1. Suppression of Electrophoresis by Alginate

Alginate's suppression of migration (i.e., electrophoresis) is illustrated in Figure 1. In the initial experiment, three gels were poured from low melting agarose (LM-agarose) or a blend of LM-agarose plus sodium alginate. For each gel, protein markers (designated "M" in Fig. 1a) were loaded in the left lane and a fluorescently-labeled antibody (designated "A") was loaded in the right lane. After electrophoresis (1 V mm^{-1} for 30 min), the gels were imaged using bright field (upper panel) and fluorescence (lower panel). For the alginate-rich gel at the left in Figure 1a, no migration of the protein markers and the labeled antibody is apparent. Results for the middle gel show substantial protein migration through an LM-agarose gel (1%) containing a small amount of alginate (0.2%). As expected, rapid protein migration was observed in the control LM-agarose gel at the right. The results

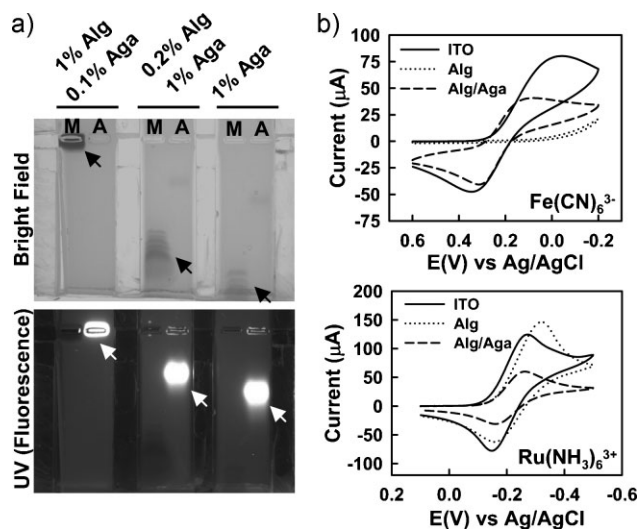


Figure 1. Alginate suppresses protein electrophoresis. a) Gel electrophoresis. Gels were prepared with differing levels of alginate (alg) and low melting agarose (aga), and electrophoresis was performed with either protein markers (M in left lanes; $10 \mu\text{g}$) or fluorescently labeled antibody (A in right lanes; Alexa Fluor 594-labeled anti-hemagglutinin; $5 \mu\text{g}$) in standard electrophoresis buffer (25 mM Tris, 250 mM Glycine; pH 8.3) at 1 V mm^{-1} for 30 min. b) CVs. Alginate or alginate-agarose films were electrodeposit onto ITO-coated slides and probed using either the negatively charged $\text{K}_3\text{Fe}(\text{CN})_6$ or the positively charged $\text{Ru}(\text{NH}_3)_6\text{Cl}_3$ (2.5 mM probe with 50 mM KCl and 50 mM phosphate buffer pH 7.0). Scan rate 50 mV s^{-1} .

in Figure 1a demonstrate that alginate suppresses protein electrophoresis.

Electrochemical methods were used to examine the suppression of electrophoresis by alginate. Specifically, separate alginate and alginate–agarose films were electrodeposited onto indium tin oxide (ITO)-coated glass slides (0.6 cm^2) and the behavior of these films was compared. Alginate was electrodeposited from a suspension containing sodium alginate (1%) and CaCO_3 (0.25%) using a constant anodic current density (4 A m^{-2}) for 2 min. The alginate–agarose film was electrodeposited from a blend of sodium alginate (0.2%), LM-agarose (1%), and CaCO_3 (0.25%) at an anodic current density of 4 A m^{-2} for 10 s. While further details of electrodeposition are provided below (and in Fig. S1 of the Supporting Information), we should note that no buffer or added salt are included in the deposition suspensions and different deposition times were used to obtain films of comparable thickness ($3.5\text{ }\mu\text{m}$ for dried alginate and $4.0\text{ }\mu\text{m}$ for dried alginate–agarose). The upper plot in Figure 1b shows cyclic voltammograms (CVs) using the anionic probe $\text{Fe}(\text{CN})_6^{3-}$. Compared to the uncoated ITO, the peak currents for this negatively charged probe are lower with the alginate–agarose film and completely suppressed with the alginate film. The lower plot in Figure 1b shows CVs using the cationic probe $\text{Ru}(\text{NH}_3)_6^{3+}$. The peak currents with this positively charged probe are lower with the alginate–agarose film but not with the alginate film. These results suggest that electrostatic repulsions are responsible (at least in part) for alginate's suppression of the electrophoresis of negatively charged proteins (further support for the role of electrostatic repulsions is provided from electrochemical impedance spectroscopy as shown in Fig. S2 in the Supporting Information).

2.2. Co-deposition of Alginate and Agarose

The co-deposition of alginate and agarose was examined using both in situ and ex situ electrochemical quartz crystal microbalance (EQCM) measurements (a schematic of the EQCM cell is provided in Fig. S3 in the Supporting Information). For in situ EQCM experiments, the quartz crystals were immersed in polysaccharide-containing solutions that were low in concentration (deposition from concentrated polysaccharide solutions exceeded the limits for in situ mass measurements) and warm ($37\text{ }^\circ\text{C}$; to ensure LM-agarose remained soluble). Anodic deposition was initiated by applying a constant voltage ($+2.5\text{ V}$) to the working electrode that was patterned on the crystal and the change in resonant frequency of the crystal was monitored over time.

In situ EQCM results from several solutions are shown in Figure 2a (solution compositions are provided in legend). For solutions lacking alginate, little change in resonant frequency is observed, which is consistent with the expectation that neither CaCO_3 nor agarose can electrodeposit. The resonant frequency for the crystal immersed in the solution containing alginate and CaCO_3 decreased monotonically with time indicating the accumulation of mass on the anode (the 60 Hz decrease in resonant frequency corresponds to 84 ng). This result is in agreement with the visual observation that a thin hydrogel film is formed on the electrode surface. Finally, Figure 2a shows an even larger decrease in resonant frequency ($\sim 200\text{ Hz}$ corresponding to

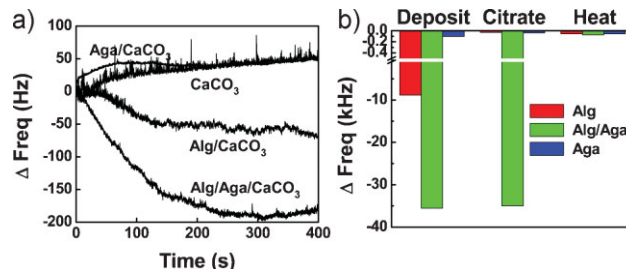


Figure 2. Co-deposition of alginate–agarose film. a) Alginate allows electrodeposition. In situ EQCM measurements indicate deposition occurs from solutions containing alginate (0.02%) or a blend of alginate (0.02%) plus LM-agarose (0.1%), while no deposition is evident for LM-agarose (0.1%) (all solutions contained 0.006% CaCO_3). b) Agarose confers thermal-responsiveness. Ex situ EQCM measurements with cooled and dried films show i) deposition occurs from a solution of alginate (0.2%) or a blend of alginate (0.2%) plus LM-agarose (1.0%), but not from a solution of LM-agarose (1.0%) (all solutions contained 0.25% CaCO_3), ii) sodium citrate (50 mM for 10 min) solubilizes alginate but not alginate–agarose films, and iii) hot water treatment ($80\text{ }^\circ\text{C}$ for 20 min) solubilizes alginate–agarose film. Ex situ EQCM measurements are referenced to the resonant frequency of quartz crystal prior to deposition.

280 ng) for deposition from a blend of alginate, LM-agarose, and CaCO_3 . Visually, a thicker film was observed to electrodeposit when LM-agarose was added to the alginate solution. The results in Figure 2a suggest that alginate allows for the co-deposition of LM-agarose—presumably the agarose chains are entrapped within the electrodeposited alginate network.

Ex situ EQCM measurements were performed to demonstrate that agarose's thermally responsive properties are retained upon co-deposition with alginate. Deposition was performed from warm polysaccharide solutions ($37\text{ }^\circ\text{C}$; $+2.5\text{ V}$ for 1 min) after which the films were cooled (to allow the LM-agarose network to form) and dried at room temperature, and the resonant frequency was measured in air. The results at the left in Figure 2b indicate that alginate electrodeposits in the presence or absence of LM-agarose. Further, the difference in resonant frequency indicates that more mass is deposited from the polysaccharide blend than for the alginate solution ($49.8\text{ vs. }12.4\text{ }\mu\text{g}$).

Next, the crystals with the deposited films were immersed in a solution containing sodium citrate to disrupt the calcium alginate network. The ex situ EQCM measurement for the crystal with deposited alginate shows that the resonant frequency returns to the initial value (prior to deposition), which is consistent with the visual observation that calcium alginate films dissolve in sodium citrate. In contrast, both visual observation and the EQCM measurements show that the deposited film obtained from the alginate–agarose blend does not dissolve in citrate. Presumably, the thermally responsive agarose network is responsible for retention of this hydrogel film. Finally, the crystals were incubated in hot water. Visually, the alginate–agarose film was observed to dissolve and this observation is consistent with the ex situ EQCM measurements. In summary, the EQCM results indicate that alginate allows the co-deposition of warm LM-agarose and this electrodeposited blend forms a thermally responsive network upon cooling.

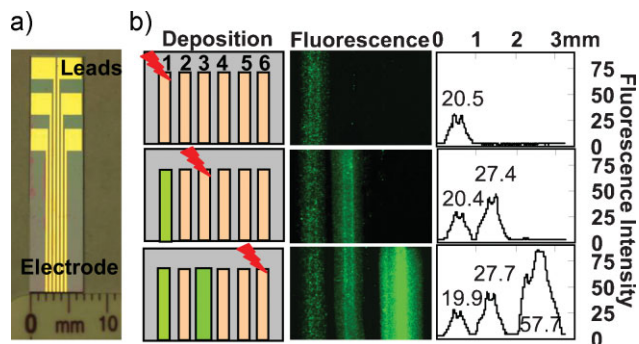


Figure 3. Spatiotemporal selectivity of alginate–agarose co-deposition. a) Photograph of chip with patterned electrode addresses. b) Sequential deposits from three separate solutions each containing 0.2% alginate but increasing LM-agarose: 0% for electrode #1, 0.5% for electrode #3, and 1.0% for electrode #6. Fluorescently labeled microparticles and CaCO_3 (0.25%) were included in all deposition solutions and deposition was performed by biasing a single electrode for 8 s at 20 A m^{-2} . Averaged fluorescence intensities are listed for each deposit.

2.3. Spatial Selectivity of Alginate–Agarose Co-deposition

One advantage of electrodeposition is that it provides a simple and rapid method for the spatiotemporally controlled assembly of hydrogel films. To illustrate this capability, we used the chip in Figure 3a and sequentially electrodeposited films onto different electrode addresses (each address is $250\text{-}\mu\text{m}$ -wide gold line spaced $250\text{-}\mu\text{m}$ apart). The deposition sequence illustrated in Figure 3b was i) deposit from alginate (0.2%) onto electrode #1, ii) deposit from an alginate (0.2%) plus LM-agarose (0.5%) blend onto electrode #3, and iii) deposit from an alginate (0.2%) plus LM-agarose (1.0%) blend onto electrode #6. Fluorescently labeled microparticles and CaCO_3 (0.25%) were included in all deposition solutions and deposition at the individual electrodes was achieved by biasing the single electrode for 8 s at a current density of 20 A m^{-2} (typically the voltage did not exceed 2.5 V). After each deposition step, the chip was cooled to room temperature and imaged using a fluorescence microscope.

Several observations are apparent from the fluorescence photomicrographs and associated image analysis shown in Figure 3b. First, electrodeposition is achieved with high spatial and temporal control. Second, the addition of LM-agarose to the blend led to increases in both fluorescence intensity and width of the deposited film which suggests that thicker films are deposited from the alginate–agarose blend. Profilometry measurements of films from various experiments indicate that the thickness of the dried films ranged from 0.5 to $2.5 \mu\text{m}$ with a consistent trend that thicker films were deposited from the blend. Third, and most importantly, Figure 3b shows that the average fluorescence image intensity of a deposited film is not altered by subsequent deposition steps indicating that each deposition step can be performed independently without disruption of previously-deposited films.

2.4. Co-deposition and Cultivation of Yeast

The model biological system for this study is a yeast strain that has been engineered to display on the cell surface a variable

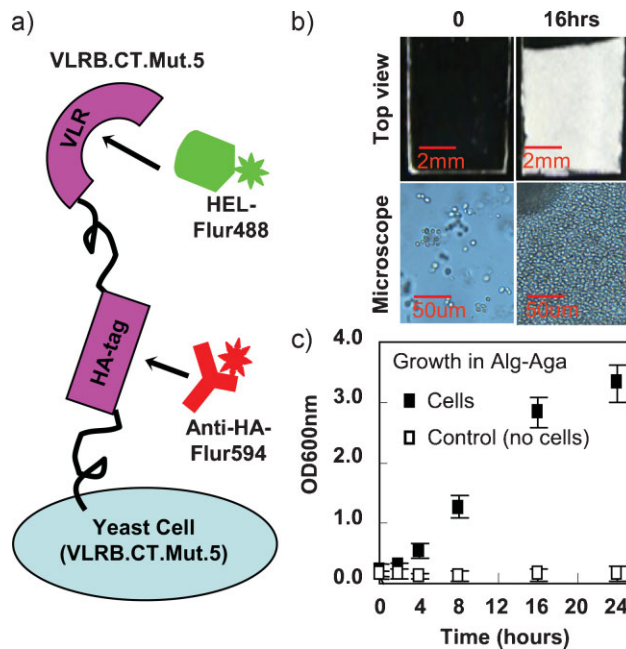


Figure 4. Yeast growth in alginate–agarose film. a) Yeast (VLRB.CT.Mut.5) model. The HEL-specific VLR with HA sequence is displayed on the cell surface. b) Photographs and photomicrographs of film grown yeast. Images obtained 0 or 16 h after electrodeposition onto an ITO-coated glass slide (2 A m^{-2} for 1 min) from a solution containing alginate (0.2%), agarose (1.0%), CaCO_3 (0.25%), and yeast (0.2 optical density). Cells were incubated in YPD growth medium. c) Growth curve for film-cultivated yeast. Yeast entrapped in several alginate–agarose films were incubated in YPD growth medium and the cells were released from an individual film to measure the optical density at 600 nm ($\text{OD}_{600\text{nm}}$).

lymphocyte receptor (VLR) from sea lamprey. VLRs are unique proteins that serve as antigen receptors in the adaptive immune system of jawless vertebrates.^[76,77] Since VLRs are assembled by recombinatorial DNA rearrangements and can recognize and bind any nominal antigen, they are functionally analogous to mammalian antibodies.^[78] However, VLRs are structurally different from antibodies, consisting of leucine-rich repeat units instead of immunoglobulins, and this difference has sparked considerable fundamental and technological interest.^[79,80] Recently, VLRs that bind the model protein hen egg lysozyme (HEL) were selected from libraries constructed in a novel yeast surface-display vector, where the VLRs were N-terminally fused to a yeast surface anchor, separated by a spacer encoding a hemagglutinin (HA) tag (Fig. 4a). The antigen-binding properties of several clones were rationally engineered by directed evolution for enhanced affinity and the clone with the most improved HEL binding ability (improved from $K_D = 155 \text{ nm}$ to $K_D = 119 \text{ }\mu\text{m}$) was designated clone VLRB.CT.Mut.5.^[78] This clone was chosen as the model in our study. This biological model is convenient because it allows inducible expression of monoclonal VLRs on the yeast surface, and the displayed protein can be detected by binding of both the HEL antigen ($\sim 15 \text{ kDa}$) and the much larger immunoreagent anti-hemagglutinin (anti-HA; $\sim 150 \text{ kDa}$).

Initial experiments demonstrate that the yeast can proliferate in electrodeposited alginate–agarose films. In these experiments, the warm suspension containing yeast (optical density 0.2), alginate

(0.2%), LM-agarose (1.0%), and CaCO_3 (0.25%) was electrodeposited (2 A m^{-2} for 1 min) onto an ITO-coated glass microscope slide. After deposition, the films were rinsed with warm water (37°C) and then briefly immersed in cold YPD (yeast, peptone, dextrose) growth medium (4°C) to allow the agarose gels to form. The upper images in Figure 4b are photographs of the film immediately following electrodeposition and after overnight incubation at 30°C . As evident from these photographs, the film became considerably more opaque during cultivation due to growth of the yeast. The lower images in Figure 4b are photomicrographs that further indicate extensive growth of the yeast during the overnight incubation.

A growth curve for yeast in the electrodeposited films was obtained by generating several films on ITO-coated glass slides as described above and harvesting individual films after specific incubation times. The yeast entrapped in the harvested films were liberated using citrate (25 mM) and a commercial chaotropic solution known to solubilize LM-agarose gels. After releasing the yeast from the films, the cells were centrifuged, washed, re-suspended in water, and the optical density of the resulting suspension was measured at 600 nm . The results in Figure 4c show substantial increases in optical density for the films “inoculated” with yeast, while control films deposited without yeast show no change in optical density. The doubling time for the entrapped yeast was estimated to be 3 h, which is comparable to the doubling time of suspension cultured yeast. Thus, yeast co-deposited and entrapped within the alginate–agarose blend can proliferate in these films (similar observations are presented in Fig. S4 of the Supporting Information for yeast entrapped in alginate films).

The experiment outlined in Figure 5a was performed to demonstrate that film cultivated yeast (VLRB.CT.Mut5) can be induced to express and display VLR protein. Specifically, yeast were co-deposited, the slides were incubated for 3 h in the YPD growth medium, and then transferred to the YPG induction medium for 16 h. To analyze VLR expression, the cells were released from the films with citrate and chaotropic solution, collected by centrifugation, washed, and suspended in phosphate buffered saline (PBS) buffer (10 mM phosphate; 150 mM NaCl; pH 7.4). To detect VLR expression, the released cells were first incubated with the labeled HEL antigen (100 nM in PBS for 1 h), washed, and then incubated with labeled anti-HA antibody ($5 \mu\text{g mL}^{-1}$ in PBS for 1 h). The images from confocal laser scanning microscopy are shown in Figure 5b. These images indicate considerable green fluorescence (left image; indicating HEL binding), red fluorescence (center image; indicating anti-HA binding), and co-localization of the fluorescence (right image; suggesting the antigen and anti-HA binding sites are on the same yeast). Little fluorescence was observed for non-induced control cells (data not shown). Thus, the images in Figure 5b indicate that film-cultivated yeast can be induced to express VLR. Confocal images at higher magnification are shown in Figure 5c. These images also show co-localization of the green and red fluorescence and further suggest that the VLR is displayed on the yeast surface.

A time-course for VLR induction was obtained by co-depositing yeast onto several ITO-coated slides and harvesting individual samples after specified times post-induction. For analysis, the yeast were released from the film, incubated simultaneously with labeled HEL antigen (100 nM) and labeled anti-HA ($5 \mu\text{g mL}^{-1}$) for

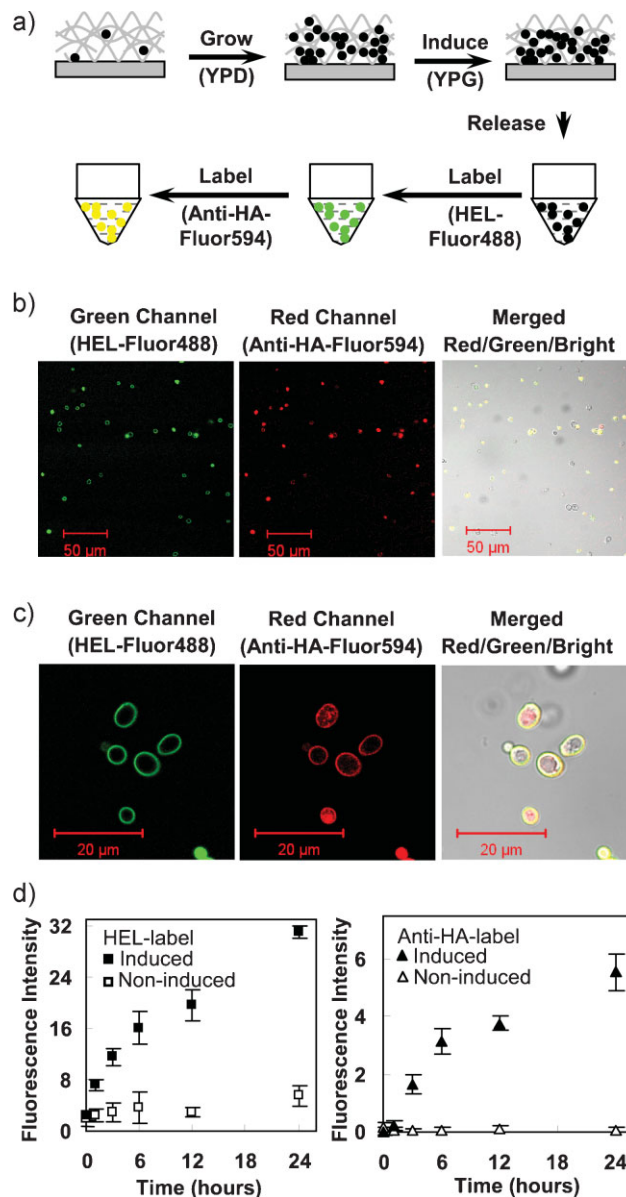


Figure 5. Induction of VLR expression and surface display in film-cultured yeast. a) Sequence to grow, induce, release, and analyze VLR expression of film-cultured yeast. b) Confocal images of induced yeast. Green fluorescence indicates binding of fluorescently labeled HEL antigen; red fluorescence indicates binding of anti-HA antibody; and yellow fluorescence in the merged image indicates co-localization of green and red fluorescence. c) High-magnification confocal images suggest VLR display on yeast surface. d) Induction curves for film-cultivated yeast. Binding of the fluorescently labeled HEL antigen and the anti-HA immunoreagent was measured after the yeast were released from the alginate–agarose films.

1 h, washed, and then measured using a fluorescence plate reader. The plots in Figure 5d indicate a steady and simultaneous increase in both green and red fluorescence consistent with the expression of VLR. Figure 5d also shows minimal fluorescence for the non-induced controls. (Fig. S5 of the Supporting Information shows that the induction of VLR expression by yeast entrapped in alginate

films is similar to that for cells entrapped within the alginate-agarose blend.)

2.5. Immunoanalysis of Entrapped Yeast

Finally, we demonstrate immunoanalysis of the entrapped VLRB.CT.Mut5 yeast using the experimental procedure illustrated in Figure 6a. In this experiment, bovine serum albumin (BSA; 1.0%) was included in the deposition solution to limit non-specific binding during the subsequent immunoanalysis. After deposition, the slides were incubated in YPD growth medium (3 h) and then YPG induction medium (4 h). After induction, the slides were rinsed and incubated with a Tris buffer (50 mM; pH 7.5) containing the fluorescently labeled HEL antigen (100 nM for 1 h), and then rinsed and incubated with fluorescently labeled anti-HA antibody (5 $\mu\text{g mL}^{-1}$ in Tris for 1 h).

The micrographs in Figure 6b for the non-induced control show no fluorescence with either the green filter (labeled-HEL antigen) or red filter (labeled anti-HA) consistent with the absence of surface displayed VLR. The induced culture in Figure 6b shows considerable fluorescence with the green filter indicating that the small (~ 15 kDa) and basic (pI ~ 11) HEL antigen can diffuse into the alginate-agarose film and bind to the VLR. However, little fluorescence was observed using the red filter suggesting that the larger and more acidic anti-HA antibody has limited ability to diffuse into the hydrogel network.

We next examined the use of electrophoresis to enable the anti-HA immunoreagent to penetrate the film and access the entrapped yeast. In this study, the yeast were electrodeposited, grown, induced and contacted with the labeled HEL antigen as described above. Next the slides were inserted into the electrophoresis device shown in Figure 6c with a platinum foil serving as the counter electrode. Electrophoresis was performed by adding labeled anti-HA (5 $\mu\text{g mL}^{-1}$) to the electrophoresis buffer and applying an electric field of 1 V mm^{-1} for 20 min (ITO coated slide served as the positive electrode). The green fluorescence image at the top left in Figure 6d is consistent with the binding of the HEL antigen to cells. The middle image at the top in Figure 6d shows red fluorescence is observed throughout the field indicating that the labeled anti-HA antibody has penetrated into the film due to the applied electric field. This observation is consistent with Figure 1a, which shows that proteins can readily migrate through a gel prepared from alginate (0.2%) and LM-agarose (1%).

A second sample was prepared by performing two electrophoresis steps. Initially an electric field of 1 V mm^{-1} was applied for 20 min (ITO-coated slide served as the positive electrode) to drive the anti-HA into the film. After replacing the solution with protein-free electrophoresis buffer, a second electrophoresis step was performed at 1 V mm^{-1} for 30 min in the opposite direction (the ITO-coated slide served as the negative electrode) to remove unbound anti-HA from the film. The fluorescence images at the bottom in Figure 6d show that red fluorescence is observed in localized regions and these regions are co-localized with the green fluorescence obtained from the labeled HEL antigen. In conclusion, Figure 6 shows that cells electrodeposited in the alginate-agarose films can be probed using the electrophoresis of immunoreagents (i.e., antibodies) to examine the proteins

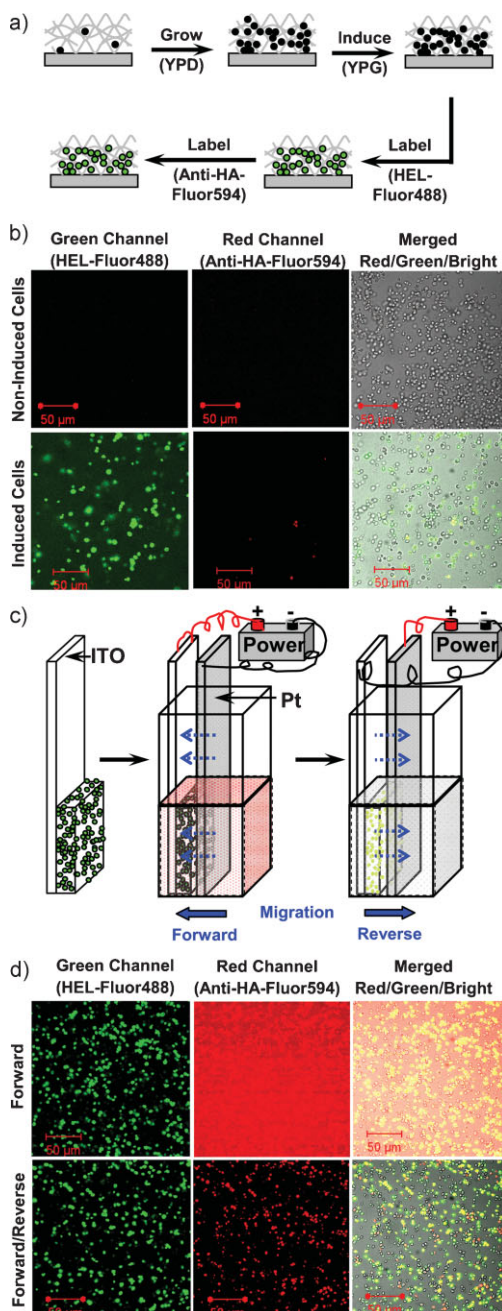


Figure 6. Detection of surface displayed proteins for film-entrapped yeast. a) Sequence to grow, induce, and analyze entrapped yeast in the absence of electrophoresis. b) Confocal images of film-entrapped yeast immunoanalyzed without electrophoresis. No fluorescence is observed for non-induced control cells while induced cells show green fluorescence (HEL binding) but not red fluorescence (anti-HA binding). Presumably the larger and more acidic anti-HA protein cannot diffuse into the alginate-agarose film. c) Schematic of electrophoresis approach to contact entrapped yeast with anti-HA. Forward electrophoresis step drives antibody into the alginate-agarose film (1 V mm^{-1} for 20 min) while the reverse step removes unbound anti-HA antibody from the film (1 V mm^{-1} for 30 min). d) Confocal images of film-entrapped yeast immunoanalyzed with electrophoresis. Entrapped cells were first contacted with labeled HEL antigen. Then, the entrapped cells were contacted with labeled anti-HA with forward electrophoresis only (upper images) or forward plus reverse electrophoresis (bottom images).

displayed on their surface. (Fig. S6 in the Supporting Information demonstrate that yeast co-deposited with alginate (without agarose) cannot be probed with the anti-HA immunoreagent.)

3. Conclusions

These studies demonstrate that low levels of alginate allow for the co-deposition of other, stimuli-responsive biopolymers (i.e., agarose) and this observation should extend the utility of electrodeposition in two ways. First, it enables the co-deposition of polymers that can form films in response to additional stimuli (rather than simply a pH gradient). Second, it extends deposition to neutral polymers that allow access to a broader range of biotechnological procedures (e.g., electrophoresis). From a device perspective, electrodeposition with stimuli-responsive biopolymers is potentially significant because it enlists convenient electrical signals for programmable assembly.^[43,81,82] From a biology perspective, electrodeposition provides a rapid, reagentless, and biocompatible means to electroaddress viable biological materials.^[51,83] The ability to couple electrodeposition with in-film bioprocessing and immunoanalysis could enable applications that include evaluating biopsy samples for enhanced diagnosis and personalized medicine,^[84] providing experimental systems for studying multi-organ drug metabolism to facilitate discovery and toxicity testing,^[2] and creating the spatially controlled environments that provide key developmental cues (e.g., for tissue engineering).^[14]

4. Experimental

The following chemicals were purchased from Sigma-Aldrich: sodium alginate from brown algae (medium viscosity), calcium carbonate power (10 μm), PBS (pH 7.4), FITC-labeled microparticles based on melamine resin (1 μm), ITO-coated glass slides (surface resistivity 8–12 Ωsq^{-1}), $\text{K}_3\text{Fe}(\text{CN})_6$, $\text{Ru}(\text{NH}_3)_6\text{Cl}_3$, and HEL (14.7 kDa; pI \sim 11). Additional chemicals were purchased including LM-agarose (Promega), tris(hydroxymethyl)aminomethane (Tris; Fischer), NHS-fluorescein (Pierce), red-fluorescent Alexa Fluor 594 anti-HA antibody (Invitrogen), and protein markers (EZ-Run Pre-Stained RecProtein Ladder; Fisher Scientific). The commercial chaotropic solution (4.5 M isothiocyanate, 0.5 M acetate, pH 5) used was the “membrane binding solution” from Wizard SV Gel and PCR Clean-up System (Promega).

The YPD growth medium contains Bacto yeast extract (10 g L^{-1}), Bacto proteose peptone (20 g L^{-1}), dextrose (i.e., glucose; 20 g L^{-1}) and the antibiotic geneticin (G418; 100 $\mu\text{g mL}^{-1}$). The YPG (yeast, peptone, galactose) induction medium contains Bacto yeast extract (10 g L^{-1}), Bacto proteose peptone (20 g L^{-1}), galactose (20 g L^{-1}), and the antibiotic geneticin (G418; 100 $\mu\text{g mL}^{-1}$). Unless otherwise noted, yeast were co-deposited from a warm suspension containing yeast (optical density 0.2), alginate (0.2%), LM-agarose (1.0%), and CaCO_3 (0.25%) onto an ITO-coated glass microscope slide using a constant current density (2 A m^{-2}) for 1 min.

Several standard experimental methods were used in this study. Chips were prepared using conventional microfabrication methods to pattern gold onto silicon wafers. HEL was fluorescently labeled with NHS-fluorescein using a standard labeling kit and instructions provided by the supplier (Pierce NHS-Fluorescein Antibody Labeling Kit). Image analysis of the fluorescence photomicrographs of the electrodeposited microparticles on the patterned chip was performed using Image J software. Electrophoresis was performed using standard electrophoresis buffer composed of 25 mM Tris and 250 mM Glycine (pH 8.3). Changes in the

resonant frequency measured with the quartz crystal microbalance were converted into mass changes using the Sauerbrey equation.

The following instruments were used in this study: spectrophotometer (Thermo Scientific, Evolution60), electrochemical analyzer (CH Instruments), electrochemical quartz crystal microbalance (EQCM; CH Instruments), fluorescence plate reader (SpectraMax M2 Microplate Readers), confocal laser scanning microscope (Zeiss, LSM510 meta), fluorescence microscope (Leica MZ FLIII, with GFP2 filter), profilometer (Alpha-step 500 Surface Profiler, TENCOR Instruments), and power supply (Keithley, 2400 sourcemeter).

Acknowledgements

The authors gratefully acknowledge financial support from the R.W. Deutsch Foundation, the National Science Foundation (NSF; EFRI-0735987), and the Department of Defense, Defense Threat Reduction Agency (W91B9480520121). Supporting Information is available online from Wiley InterScience or from the author.

Received: November 6, 2009

Published online: April 23, 2010

- [1] W. P. Daley, S. B. Peters, M. Larsen, *J. Cell Sci.* **2008**, *121*, 255.
- [2] J. H. Sung, M. L. Shuler, *Lab Chip* **2009**, *9*, 1385.
- [3] M. C. Cushing, K. S. Anseth, *Science* **2007**, *316*, 1133.
- [4] N. W. Choi, M. Cabodi, B. Held, J. P. Gleghorn, L. J. Bonassar, A. D. Stroock, *Nat. Mater.* **2007**, *6*, 908.
- [5] I. Tokarev, V. Gopishetty, J. Zhou, M. Pita, M. Motornov, E. Katz, S. Minko, *ACS Appl. Mater. Interfaces* **2009**, *1*, 532.
- [6] I. Tokarev, S. Minko, *Soft Matter* **2009**, *5*, 511.
- [7] I. Tokarev, S. Minko, *Adv. Mater.* **2009**, *21*, 241.
- [8] M. M. Stevens, M. Mayer, D. G. Anderson, D. B. Weibel, G. M. Whitesides, R. Langer, *Biomaterials* **2005**, *26*, 7636.
- [9] Z. H. Nie, E. Kumacheva, *Nat. Mater.* **2008**, *7*, 277.
- [10] A. Khademhosseini, R. Langer, *Biomaterials* **2007**, *28*, 5087.
- [11] D. B. Weibel, W. R. DiLuzio, G. M. Whitesides, *Nat. Rev. Microbiol.* **2007**, *5*, 209.
- [12] T. H. Park, M. L. Shuler, *Biotechnol. Prog.* **2003**, *19*, 243.
- [13] H. Tavana, A. Jovic, B. Mosadegh, Q. Y. Lee, X. Liu, K. E. Luker, G. D. Luker, S. J. Weiss, S. Takayama, *Nat. Mater.* **2009**, *8*, 736.
- [14] L. Grossin, D. Cortial, B. Saulnier, O. Felix, A. Chassepot, G. Decher, P. Netter, P. Schaaf, P. Gillet, D. Mainard, J. C. Voegel, N. Benkirane-Jessel, *Adv. Mater.* **2009**, *21*, 650.
- [15] T. R. Colbourne, I. G. Hill, L. Kreplak, *Biomacromolecules* **2009**, *10*, 1986.
- [16] H. R. Baker, E. F. Merschrod, K. A. Poduska, *Langmuir* **2008**, *24*, 2970.
- [17] M. Gabi, T. Sannomiya, A. Larmagnac, M. Puttaswamy, J. Voros, *Integr. Biol.* **2009**, *1*, 108.
- [18] T. Geng, N. Bao, O. Z. Gall, C. Lu, *Chem. Commun.* **2009**, 800.
- [19] D. R. Albrecht, G. H. Underhill, A. Mendelson, S. N. Bhatia, *Lab Chip* **2007**, *7*, 702.
- [20] K. C. Wood, N. S. Zacharia, D. J. Schmidt, S. N. Wrightman, B. J. Andaya, P. T. Hammond, *Proc. Natl. Acad. Sci. U. S. A.* **2008**, *105*, 2280.
- [21] Y. H. Bai, J. J. Xu, H. Y. Chen, *Biosens. Bioelectron.* **2009**, *24*, 2985.
- [22] B. P. Corgier, C. A. Marquette, L. J. Blum, *J. Am. Chem. Soc.* **2005**, *127*, 18328.
- [23] B. P. Corgier, C. A. Marquette, L. J. Blum, *Biosens. Bioelectron.* **2007**, *22*, 1522.
- [24] R. Polsky, J. C. Harper, S. M. Dirk, D. C. Arango, D. R. Wheeler, S. M. Brozik, *Langmuir* **2007**, *23*, 364.
- [25] R. Polsky, J. C. Harper, D. R. Wheeler, S. M. Dirk, D. C. Arango, S. M. Brozik, *Biosens. Bioelectron.* **2008**, *23*, 757.
- [26] H. Kaji, M. Hashimoto, M. Nishizawa, *Anal. Chem.* **2006**, *78*, 5469.

- [27] P. M. Mendes, K. L. Christman, P. Parthasarathy, E. Schopf, J. Ouyang, Y. Yang, J. A. Preece, H. D. Maynard, Y. Chen, J. F. Stoddart, *Bioconjugate Chem.* **2007**, *18*, 1919.
- [28] I. Y. Wong, M. J. Footer, N. A. Melosh, *Soft Matter* **2007**, *3*, 267.
- [29] K. Kim, J. Hwang, I. Seo, T. H. Youn, J. Kwak, *Chem. Commun.* **2006**, 4723.
- [30] K. Kim, M. Jang, H. S. Yang, E. Kim, Y. T. Kim, J. Kwak, *Langmuir* **2004**, *20*, 3821.
- [31] K. Kim, H. Yang, S. Jon, E. Kim, J. Kwak, *J. Am. Chem. Soc.* **2004**, *126*, 15368.
- [32] W. S. Yeo, M. N. Yousaf, M. Mrksich, *J. Am. Chem. Soc.* **2003**, *125*, 14994.
- [33] S. Cosnier, *Biosens. Bioelectron.* **1999**, *14*, 443.
- [34] L. Q. Wu, G. F. Payne, *Trends Biotechnol.* **2004**, *22*, 593.
- [35] S. Ladet, L. David, A. Domard, *Nature* **2008**, *452*, 76.
- [36] A. K. Manocchi, P. Domachuk, F. G. Omenetto, H. M. Yi, *Biotechnol. Bioeng.* **2009**, *103*, 725.
- [37] A. L. Paguirigan, D. J. Beebe, *Nat. Protoc.* **2007**, *2*, 1782.
- [38] A. P. Wong, R. Perez-Castillejos, J. C. Love, G. M. Whitesides, *Biomaterials* **2008**, *29*, 1853.
- [39] R. M. Johann, P. Renaud, *Biointerphases* **2007**, *2*, 73.
- [40] J. A. Rowley, G. Madlambayan, D. J. Mooney, *Biomaterials* **1999**, *20*, 45.
- [41] T. Chen, D. A. Small, M. K. McDermott, W. E. Bentley, G. F. Payne, *Biomacromolecules* **2003**, *4*, 1558.
- [42] L. Q. Wu, A. P. Gadre, H. M. Yi, M. J. Kastantin, G. W. Rubloff, W. E. Bentley, G. F. Payne, R. Ghodssi, *Langmuir* **2002**, *18*, 8620.
- [43] H. M. Yi, L. Q. Wu, W. E. Bentley, R. Ghodssi, G. W. Rubloff, J. N. Culver, G. F. Payne, *Biomacromolecules* **2005**, *6*, 2881.
- [44] R. Fernandes, L. Q. Wu, T. H. Chen, H. M. Yi, G. W. Rubloff, R. Ghodssi, W. E. Bentley, G. F. Payne, *Langmuir* **2003**, *19*, 4058.
- [45] X. Pang, I. Zhitomirsky, *Mater. Chem. Phys.* **2005**, *94*, 245.
- [46] R. A. Zangmeister, J. J. Park, G. W. Rubloff, M. J. Tarlov, *Electrochim. Acta* **2006**, *51*, 5324.
- [47] M. Cheong, I. Zhitomirsky, *Colloids Surf. A* **2008**, *328*, 73.
- [48] C. H. Liu, X. L. Guo, H. T. Cui, R. Yuan, *J. Mol. Catal. B: Enzym.* **2009**, *60*, 151.
- [49] F. Sun, I. Zhitomirsky, *Surf. Eng.* **2009**, *25*, 621.
- [50] K. Grandfield, F. Sun, M. FitzPatrick, M. Cheong, I. Zhitomirsky, *Surf. Coat. Technol.* **2009**, *203*, 1481.
- [51] X. W. Shi, C.-Y. Tsao, X. Yang, Y. Liu, P. Dykstra, G. W. Rubloff, R. Ghodssi, W. E. Bentley, G. F. Payne, *Adv. Funct. Mater.* **2009**, *19*, 2074.
- [52] X. L. Luo, J. J. Xu, Y. Du, H. Y. Chen, *Anal. Biochem.* **2004**, *334*, 284.
- [53] X. L. Luo, J. J. Xu, Q. Zhang, G. J. Yang, H. Y. Chen, *Biosens. Bioelectron.* **2005**, *21*, 190.
- [54] Y. H. Bai, Y. Du, J. J. Xu, H. Y. Chen, *Electrochem. Commun.* **2007**, *9*, 2611.
- [55] F. Li, Z. Wang, W. Chen, S. S. Zhang, *Biosens. Bioelectron.* **2009**, *24*, 3030.
- [56] X. D. Zeng, X. F. Li, L. Xing, X. Y. Liu, S. L. Luo, W. Z. Wei, B. Kong, Y. H. Li, *Biosens. Bioelectron.* **2009**, *24*, 2898.
- [57] J. D. Qiu, R. Wang, R. P. Liang, X. H. Xia, *Biosens. Bioelectron.* **2009**, *24*, 2920.
- [58] F. N. Xi, L. J. Liu, Q. Wu, X. F. Lin, *Biosens. Bioelectron.* **2008**, *24*, 29.
- [59] X. Y. Wang, H. F. Gu, F. Yin, Y. F. Tu, *Biosens. Bioelectron.* **2009**, *24*, 1527.
- [60] Q. M. Zhou, Q. J. Xie, Y. C. Fu, Z. H. Su, X. Jia, S. Z. Yao, *J. Phys. Chem. B* **2007**, *111*, 11276.
- [61] T. Tangkuaram, C. Ponchio, T. Kangkasomboon, P. Katikawong, W. Veerasai, *Biosens. Bioelectron.* **2007**, *22*, 2071.
- [62] C. Hao, L. Ding, X. Zhang, H. Ju, *Anal. Chem.* **2007**, *79*, 4442.
- [63] J. M. Gong, L. Y. Wang, K. Zhao, D. D. Song, *Electrochem. Commun.* **2008**, *10*, 123.
- [64] X. L. Luo, J. J. Xu, J. L. Wang, H. Y. Chen, *Chem. Commun.* **2005**, 2169.
- [65] F. N. Xi, L. J. Liu, Z. C. Chen, X. F. Lin, *Talanta* **2009**, *78*, 1077.
- [66] R. P. Liang, L. X. Fan, R. Wang, J. D. Qiu, *Electroanalysis* **2009**, *21*, 1685.
- [67] Z. G. Wu, W. Feng, Y. Y. Feng, Q. Liu, X. H. Xu, T. Sekino, A. Fujii, M. Ozaki, *Carbon* **2007**, *45*, 1212.
- [68] L. Q. Wu, K. Lee, X. Wang, D. S. English, W. Losert, G. F. Payne, *Langmuir* **2005**, *21*, 3641.
- [69] J. Redepenning, G. Venkataraman, J. Chen, N. Stafford, *J. Biomed. Mater. Res. A* **2003**, *66*, 411.
- [70] D. Zhitomirsky, J. A. Roether, A. R. Boccaccini, I. Zhitomirsky, *J. Mater. Process. Technol.* **2009**, *209*, 1853.
- [71] J. Wang, J. de Boer, K. de Groot, *J. Dent. Res.* **2004**, *83*, 296.
- [72] M. Cheong, I. Zhitomirsky, *Surf. Eng.* **2009**, *25*, 346.
- [73] S. Sharma, V. P. Soni, J. R. Bellare, *J. Mater. Sci. : Mater. Med.* **2009**, *20*, 1427.
- [74] F. Sun, K. N. Sask, J. L. Brash, I. Zhitomirsky, *Colloids Surf. B* **2008**, *67*, 132.
- [75] F. Sun, X. Pang, I. Zhitomirsky, *J. Mater. Process. Technol.* **2009**, *209*, 1597.
- [76] Z. Pancer, C. T. Amemiya, G. R. Ehrhardt, J. Ceitlin, G. L. Gartland, M. D. Cooper, *Nature* **2004**, *430*, 174.
- [77] I. B. Rogozin, L. M. Iyer, L. Liang, G. V. Glazko, V. G. Liston, Y. I. Pavlov, L. Aravind, Z. Pancer, *Nat. Immunol.* **2007**, *8*, 647.
- [78] S. Tasumi, C. A. Velikovsky, G. Xu, S. A. Gai, K. D. Wittrup, M. F. Flajnik, R. A. Mariuzza, Z. Pancer, *Proc. Natl. Acad. Sci. U. S. A.* **2009**, *106*, 12891.
- [79] C. A. Velikovsky, L. Deng, S. Tasumi, L. M. Iyer, M. C. Kerzic, L. Aravind, Z. Pancer, R. A. Mariuzza, *Nat. Struct. Mol. Biol.* **2009**, *16*, 725.
- [80] Z. Pancer, R. A. Mariuzza, *Nat. Biotechnol.* **2008**, *26*, 402.
- [81] J. J. Park, X. Luo, H. Yi, T. M. Valentine, G. F. Payne, W. E. Bentley, R. Ghodssi, G. W. Rubloff, *Lab Chip* **2006**, *6*, 1315.
- [82] X. L. Luo, A. T. Lewandowski, H. M. Yi, G. F. Payne, R. Ghodssi, W. E. Bentley, G. W. Rubloff, *Lab Chip* **2008**, *8*, 420.
- [83] X. W. Shi, X. H. Yang, K. J. Gaskell, Y. Liu, E. Kobatake, W. E. Bentley, G. F. Payne, *Adv. Mater.* **2009**, *21*, 984.
- [84] S. E. Weigum, P. N. Floriano, N. Christodoulides, J. T. McDevitt, *Lab Chip* **2007**, *7*, 995.